Nonmotorized Hand Exoskeleton for Rescue and Beyond: Substantially Elevating Grip Endurance and Strength

Xianlong Mai, Jian Yang, Lei Li, Bin Zi, Shiwu Zhang, *Member, IEEE*, Xinglong Gong, Weihua Li, Guolin Yun, and Shuaishuai Sun

***Abstract*—Robotic hand exoskeletons hold immense potential for enhancing human hand functionality, addressing the hand's strength limitations and fatigue during physically-demanding tasks. However, most existing hand exoskeletons are motorized, being weak in generating high supporting force for gripping augmentation. We present a nonmotorized hand exoskeleton based on magnetorheological (MR) actuators to provide high gripping support and elevate grip endurance. Meanwhile, it ingeniously harnesses human energy for actuation and energy storage, enhancing grip strength without external power. The MR actuator demonstrates a peak holding force of 1046 N with merely 5 W power input, boasting a force-to-power ratio one-order-of-magnitude higher than conventional approaches, and 97.7% energy reduction for same holding force compared to other approaches. Participants wearing the hand exoskeletons experience a 41.8% enhancement in grip strength without external power and reduced hand muscle fatigue during prolonged physical labor. In rescuing scenarios such as postearthquake rescue, debris clearance, and casualty evacuation, our exoskeleton effectively supports gripping and improves working efficiency.**

***Index Terms*—Grip assistance, grip strength and endurance enhancement, hand exoskeleton, magnetorheological technology, wearable robot.**

Received 21 February 2025; revised 25 May 2025; accepted 29 June 2025. Date of publication 15 July 2025; date of current version 11 August 2025. This work was supported in part by the National Natural Science Foundation of China under Grant 52005474, Grant 52105081, and Grant U21A20119, in part by USTC start-up funding under Grant KY2090000067, in part by the Fundamental Research Funds for the Central Universities under Grant WK2480000009, in part by Student's Innovation and Entrepreneurship Foundation of USTC under Grant CY2022G01, and in part by the Royal Society Newton International Fellowship under Grant NIF\R1\211458. This article was recommended for publication by Associate Editor Ana Luisa Trejos and Editor Patrick M. Wensing upon evaluation of the reviewers' comments. *(Xianlong Mai and Jian Yang contributed equally to this work.) (Corresponding authors: Weihua Li; Guolin Yun; Shuaishuai Sun.)*

This work involved human subjects or animals in its research. Approval of all ethical and experimental procedures and protocols was granted by the Medical Research Ethics Committee of the First Affiliated Hospital of USTC under Application No. 2023KY239, and performed in line with the declaration of Helsinki.

Xianlong Mai, Lei Li, Shiwu Zhang, Guolin Yun, and Shuaishuai Sun are with the CAS Key Laboratory of Mechanical Behavior and Design of Materials, Institute of Humanoid Robots, School of Engineering Sciences, University of Science and Technology of China, Hefei 230026, China (e-mail: ygl@ustc.edu.cn; sssun@ustc.edu.cn).

Jian Yang is with the School of Electrical Engineering and Automation, Anhui University, Hefei 230601, China.

Bin Zi is with the School of Mechanical Engineering, Hefei University of Technology, Hefei 230009, China.

Xinglong Gong is with the CAS Key Laboratory of Mechanical Behavior and Design of Materials, Department of Modern Mechanics, University of Science and Technology of China, Hefei 230027, China.

Weihua Li is with the School of Mechanical, Materials, Mechatronic, and Biomedical Engineering, University of Wollongong, Wollongong, NSW 2522, Australia (e-mail: weihuali@uow.edu.au).

This article has supplementary downloadable material available at https://doi.org/10.1109/TRO.2025.3588750, provided by the authors.

Digital Object Identifier 10.1109/TRO.2025.3588750

I. Introduction

THE hand, a pivotal organ in human evolution, facilitates intricate tasks essential to daily life. From heavy activities like gripping, lifting, and carrying to delicate operations such as needle threading and writing, hands serve as indispensable end effectors, enabling interaction with the world. To execute those tasks, gripping is indispensable as the most fundamental function of the hand [1]. However, individuals lacking specialized training often experience hand fatigue due to limitations in forearm muscle size and strength, rendering them inadequate for prolonged or heavy-load gripping. This challenge even extends to trained professionals like rescue workers and firefighters. Therefore, enhancing gripping endurance and strength has been a long-standing goal for researchers, crucial for relieving stress on hands and arms, improving working efficiency, and reducing injury risks. Current solutions to this limitation mainly rely on hand exoskeletons.

As promising solutions to address this challenge, hand exoskeletons have been studied for rehabilitation, assistance in activities of daily living (ADL), and task-specific training over the past two decades [2], [3], [4], [5]. However, these hand exoskeletons are weak in providing high supporting force for gripping ability augmentation, which is constrained by traditional actuation technology. Existing hand exoskeletons commonly employ four actuation types [6]: DC-motor-based design [7], [8], servo-motor-based design [9], pneumatic-based design [10], and shape-memory-alloy-based (SMA-based) design [11]. While SMA-based exoskeletons offer a high power-to-volume ratio and compactness, they can only provide low response force with low response speed [12] and poor energy efficiency [13]. Pneumatically actuated exoskeletons demonstrate a high power-to-weight ratio and mechanical compliance [14], [15]. However, they require external air compression systems, typically bulky and noisy, with limited operational duration [16]. Electric motors usually include linear [17], [18], [19] and rotational [20], [21],

[22], [23], [24] motors, and are highly available and easily controllable. However, electric motors for hand exoskeletons are size-limited, and therefore, struggle to provide high output force. Electrostatic clutches offer a simple and cost-effective solution for providing highly controllable locking forces [25], [26], [27]. However, their operational principle often results in relatively high energy consumption. Additionally, they require a large contact area to generate sufficient friction force, making them challenging to integrate into hand exoskeleton designs. Each actuation type has its advantages and disadvantages, but all face the challenge of providing high gripping force to improve grip strength and endurance for hand exoskeletons. For instance, a cord-driven unpowered exoskeleton in [28] aimed to alleviate finger fatigue but showed limited effect on grip endurance. Many hand exoskeletons failed to provide sufficient holding force due to the constraint of actuators' sizes. For example, the series elastic actuators in [29] generate only 20 N of assistive force per finger, and the linear actuators reported in [30] achieve a maximum of approximately 10 N per finger. The sizes of actuators in current hand exoskeletons are constrained by the available space on the exoskeletons, restricting their output forces and ability to provide higher supporting forces. Therefore, most existing hand exoskeletons mainly facilitate ADL and rehabilitation but struggle to lift heavy objects or support human weight. Thus, developing an actuation mechanism and hand exoskeletons that not only provide substantial supporting force and effectively improve grip strength and endurance, but are also energy-efficient, is critical for the progress of hand exoskeletons, particularly for applications in rescue operations.

Recently, magnetorheological (MR) materials show increasing advantages in developing high force-to-power ratio semiactive exoskeletons [31], [32], [33]. These MR-based exoskeletons showed advantages of highly adjustable supporting force, compact structure, and lower energy consumption. MR materials are created by comprising micron-sized ferromagnetic particles into a nonmagnetic medium [34], [35], and have highly adjustable modulus under magnetic field. Widely employed in exoskeletons, prostheses, automobiles, high-speed trains, and aseismic applications, MR technology offers advantages including high adjustability of output force or torque, lightweight construction, fast response, energy efficiency, and noiselessness [36], [37], [38], [39], [40], [41], [42], [43]. Particularly, MR grease (MRG) offers long-term stability against sedimentation and self-sealing properties compared to the more commonly used MR fluid [44], [45]. These advantages stem from the high-viscosity carrier, grease, which effectively disperses magnetic particles and counteracts gravity. As a result, MRG stands out as a promising material for robotic exoskeleton design.

We present a nonmotorized and semiactive MR hand exoskeleton (MRHE) system (see Fig. 1) that can not only enhance user's grip strength solely by harnessing human energy, but also provide extremely high supporting force and significantly extend grip endurance with low energy consumption. The proposed MR actuator effectively leverages the damping characteristics of MR materials through an innovative and compact structural design, offering potential inspiration for further research on wearable robotic devices. Moreover, the experiments conducted provide new data on MR materials' performance in dynamic robotic systems, contributing to a deeper understanding of their behavior in real-world applications. Compared to previous studies [31], [32], [33], this work introduces new designs and highlights new potential applications of MR materials in exoskeleton systems. The MRHE's primary application is in rescue situations or other scenarios that demand a strong gripping force and prolonged endurance. Previous studies have explored full-body wearable robots for enhancing human performance [46], [47], [48], which could potentially be used in rescue situations. However, to the best of our knowledge, no wearable hand exoskeleton has been specifically reported for rescue applications. The proposed MR hand exoskeleton system is fully wearable, portable, and automatically controllable with long battery life. The MR actuator shows superior force-to-power ratio one-order-of-magnitude higher than conventional actuators. The following content first illustrates the design and prototype of the MR hand exoskeleton system. Then, the design and comprehensive characterizations of MR actuator are analyzed, followed by functionality evaluation of the MR hand exoskeletons in enhancing grip strength and endurance. Finally, the article conducted experiments simulating real-world applications to characterize the hand exoskeletons' practical performance in rescue scenarios.

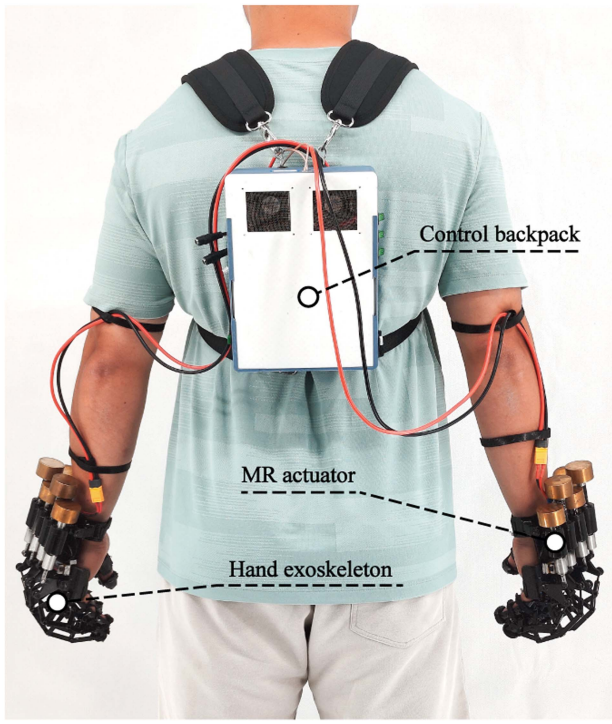

Fig. 1. System overview.

II. Mechanical Design, Working Principles, and Kinetic Model of the MRHE

A. Mechanical Design of the Hand Exoskeleton

The proposed hand exoskeleton comprises six primary physical components [see Fig. 2(a)]: 1) MR actuators for enhancement

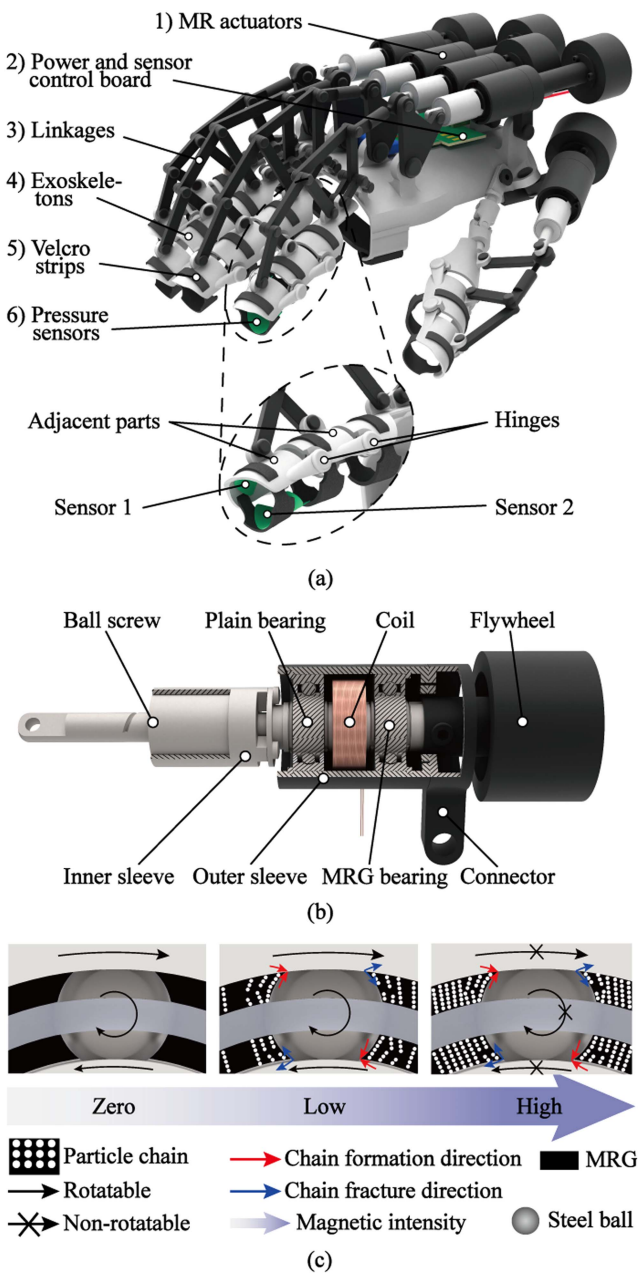

Fig. 2. Mechanical design. (a) Three-dimensional model of the hand exoskeleton prototype. The hand exoskeleton consists of six parts: 1) MR actuators; 2) power and sensor control board; 3) linkages; 4) exoskeletons; 5) Velcro strips; 6) pressure sensors. (b) Cross-sectional view of the MR actuator. (c) Three working states of the MRG bearing under different magnetic field intensities.

of grip strength and endurance; 2) a power and pressure sensor control board managing power and sensor data conversion and transmission; 3) linkages for force transmission between MR actuators and exoskeletons; 4) exoskeletons enveloping the hand; 5) Velcro strips connecting the hand to the exoskeleton; 6) two pressure sensors for grip intention detection. The hand exoskeleton works by covering back of hand and providing supporting force for the fingers. Linkages transmit forces between MR actuators and fingers. The exoskeletons are made of sintering of aluminium powder (three-dimensional printing), while the linkages are made of 7075 aluminium alloy (machining) considering structure strength for high force transmission. To ensure synchronous movement and avoid misalignment with fingers, each finger exoskeleton's adjacent parts in the design are linked via hinges that precisely aligned with respective finger joint rotational centers. Velcro strips secure fingers to the exoskeleton, ensuring synchronous movement, and accommodating various hand sizes.

B. Mechanical Design of the MR Actuator

As a key component of the hand exoskeleton, the design objectives of MR actuator are to improve grip strength, extend grip endurance, and minimize energy consumption. We introduce an innovative actuator structure [see Fig. 2(b)] comprising a ball screw, inner and outer sleeves, plain bearing, coil, MRG bearing, connector, and flywheel. Ball screws are commonly used to efficiently and precisely convert rotational motion into linear motion; however, their efficiency decreases when converting linear motion back into rotation due to ball friction. To enhance efficiency in this reverse motion, ball screws with large lead lengths (6 mm in this work) were selected, as a larger thread pitch results in a greater thread angle, reducing rotational friction in the balls. Additionally, the nut and shaft diameters were designed at 14 mm and 6 mm, respectively, to accommodate the limited space on the dorsal side of the hand. Both the inner and outer sleeves are made of low carbon steel (ASTM 1020) for higher magnetic permeability. The inner sleeve is press-fitted onto the outer surface of the nut, facilitating synchronous rotation with it. Plain and MRG bearings are positioned between the sleeves and provide radial guidance. The MRG bearing controls the rotation of inner sleeve and nut under magnetic field, thereby controlling load-bearing capacity of the MR actuator. The MRG bearing is fabricated by injecting MRG into a plain bearing (see detailed fabrication in Fig. S1). The steel balls inside the bearing are fully surrounded by MRG, as illustrated in Fig. 2(c). When the MRG bearing is exposed to a strong magnetic field, the magnetic particles in the grease form dense and robust chains, increasing the grease's shear stress and effectively locking the bearing. As the magnetic field weakens, the torque required to break the lock decreases. To achieve free rotation of the MRG bearing with minimal torque, a demagnetization method should be applied to eliminate the OFF-state effect [37]. Details of this method are provided in Fig. S2 of the Supplementary Materials.

C. Working Principles of the MRHE

Grip Strength Enhancement: In Fig. 2(b), the integration of a ball screw and flywheel on the MR actuator creates an inverter system, which accumulates human energy during gripping and generates inertial force when gripping firmly, thereby augmenting grip strength. The mechanism functions as follows: the ball screw converts the linear motion of the screw shaft into rotational motion of the nut. When the rotational damping in the MR bearing is low, the linear motion of the screw shaft is efficiently converted into rotational energy of the nut and flywheel, as shown in Fig. 3. This rotational energy can then be reconverted due to the ball screw's structure, significantly

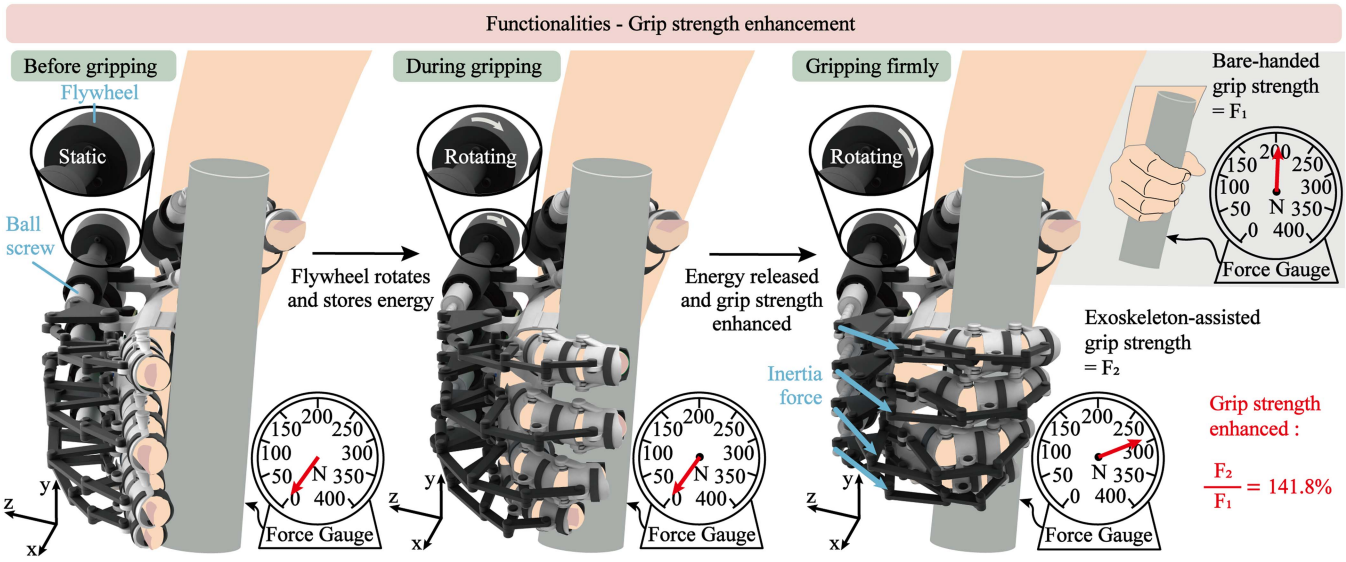

Fig. 3. Schematic illustration of grip strength enhancement solely by harnessing human energy.

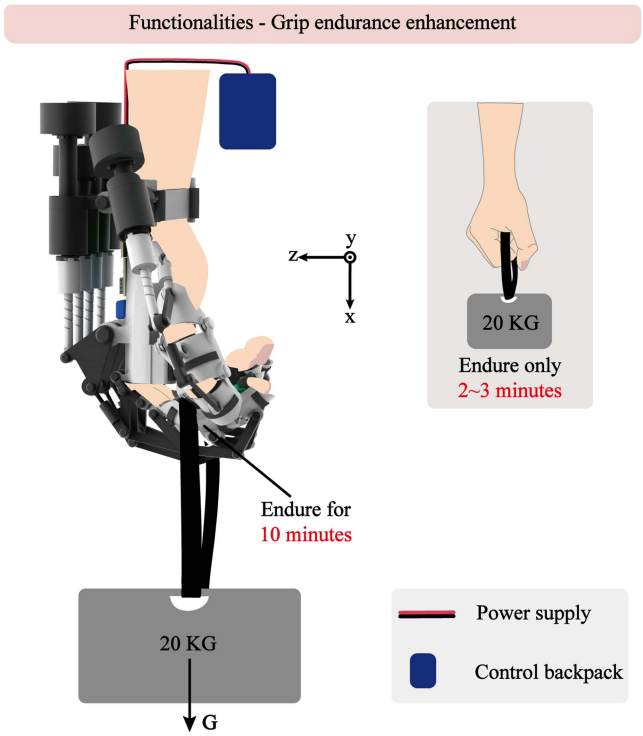

Fig. 4. Schematic illustration of grip endurance enhancement with assistance of the MRHE.

increasing the screw shaft's potential energy without requiring external actuation. This stored potential energy is subsequently used to generate a substantial inertia force on the screw shaft, thereby enhancing grip strength.

Grip Endurance Enhancement: When the rotational damping in the MR bearing is pretty high, the ball screw is locked, and the MR actuator has high load-bearing capacity. In this case, the weight on hand is supported by the MR actuator (see Fig. 4), which largely reduces the wearer's hand fatigue and enhances grip endurance.

D. Kinetic Model and Analysis of the MRHE

As is mentioned above, the ball screw converts the screw shaft's linear motion into the nut's rotation. With low resistive torque in the MRG bearing at zero magnetic level, energy of screw shaft's linear motion can be effectively harnessed as the flywheel's rotary energy. This energy transformation is reversible through the ball screw, which means the rotary energy could be converted back into the potential of screw shaft's linear motion and generation of inertia force. The rotation speeds of the sleeve and the flywheel are the same as that of the nut. According to the characteristics of the ball screw, the following relation involving the rotation speed of the nut, the lead length and velocity of the screw shaft satisfies:

$$\text{Rotation speed of the nut} \times \text{Lead of the screw shaft} = \text{Velocity of the screw shaft}.$$

In this article, the lead length of the screw shaft is 6 mm. And based on the typing investigation in [49], keystroke rates have been reported at 98–383 keys per minute for people. In this case, the average typing speed for ordinary people can be 240 keystrokes per minute. According to the research in [50], each keystroke involves the finger moving 3.3 cm back and forth on average. Then, the average finger motion speed can be calculated as 132 mm/s. Considering the resistance introduced by the exoskeleton and MR actuator, the velocity of the screw shaft in a fast grip can be 80 mm/s. Based on the above relation, it is obtained

$$n = \frac{v}{p} = 13.3\ (\mathrm{s}^{-1}) \tag{1}$$

where n is the rotation speed of the nut. v and p stand for the velocity and the lead length of the screw shaft, respectively.

According to the law of rotation, it is obtained

$$M = J \times \beta \tag{2}$$

where M is the resultant moment applied on the nut. J is the total rotary inertia from the nut, inner sleeve and flywheel. And β stands for the angular acceleration of the nut. Based on the experimental measurement in the Supplementary Method of Supplementary Materials, we set the motion stop time of the ball screw to be $\Delta t = 15$ ms, and the following equation can be obtained:

$$\beta = \frac{\omega}{\Delta t} = \frac{2\pi n}{\Delta t} = \frac{2 \times \pi \times 13.3}{0.015} \approx 5571.1 \left(\frac{\text{rad}}{\text{s}^2}\right). \tag{3}$$

From the equation of rotary inertia of cylinders

$$J = \frac{1}{2} m_i \left(R_{i1}^2 + R_{i2}^2\right) \tag{4}$$

where the m_i, R_{i1}, and R_{i2} are the mass, inner diameter, and outer diameter of cylinder *I*, respectively, the total rotary inertia of the nut, inner sleeve and flywheel is calculated as follows:

$$J = 1.64 \times 10^{-4} \ (\text{kg} \cdot \text{m}). \tag{5}$$

Based on (1), the applied resultant moment M on the nut is calculated as follows:

$$M = J \cdot \beta = 1.64 \times 10^{-4} \times 5571.1 \approx 0.9137 \ (\text{N} \cdot \text{m}). \tag{6}$$

Relationship between the resultant moment applied on the nut and the axis force generated on the screw shaft is describe as follows:

$$M = \frac{F_N \times p}{2 \times \pi \times \eta} \tag{7}$$

where F_N is the axial force on the screw shaft and η is the transmission efficiency of the ball screw. The unit of M in (7) is kgf · mm. The value of η usually varies from 0.9 to 0.98. Set $\eta = 0.94$, the axial force F_N on the screw shaft is calculated as follows:

$$F_N = 2 \times \pi \times \eta \times M \times \frac{1}{p} \approx 91.7 \ (\text{N}). \tag{8}$$

Fig. 5(a) and (b) build the kinetic model of the MR hand exoskeleton. The kinetic model is simplified as the rigid body model, which takes the exoskeletons, linkages, and output of the actuator as two-force members and each two members are connected with hinges. There are a total of 14 groups of two-force members and they are indicated using Arabic numerals from 1 to 14, as shown in Fig. 5(a). The aim of establishing this model is to analyze and calculate the force F_N, which is generated on the end of the screw shaft when a force F is applied on the middle of finger, as shown in Fig. 5(b). The applied force, *F,* is perpendicular to the member number 4. To establish the relationships among all the forces including F, T_1, T_3,T_4, T_5, T_7, T_8, T_{10}, T_{12}, and F_N, four sets of Cartesian coordinates were built in blue and named $\mathrm{x}_1o_1y_1$, $\mathrm{x}_2o_2y_2$, $\mathrm{x}_3o_3y_3$, and $\mathrm{x}_4o_4y_4$, respectively. As shown in Fig. 5(b), all of the forces are in red. Axis x_1 is parallel to the member number 4. Axes y_2, y_3, and y_4 are along the member number 1, 5, and 8, respectively. And the rest axes y_1, x_2, x_3, and x_4 are perpendicular to x_1, y_2, y_3, and y_4, respectively. The origins of the four coordinates are fixed at the hinges, which join members number 3 and 4, members number 1, 3, and 5, members number 5, 7, and 8, and members number 8, 10, and 12. All the coordinates are right-handed systems. The axis forces of the members are marked as T_i and T_i'. The index number i

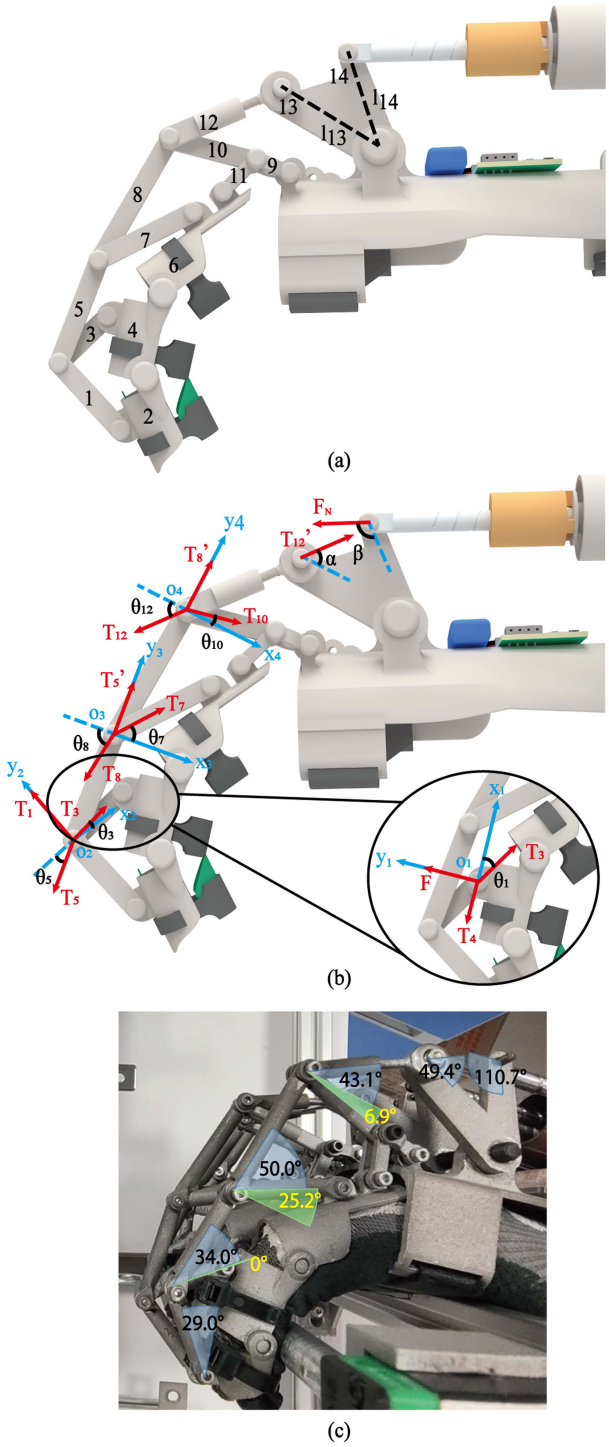

Fig. 5. Kinetic model of the MR hand exoskeleton. (a) Number of the two-force members in the kinetic model. (b) Definition of Cartesian coordinates, forces and angles related to the kinetic model. (c) Linkage angles in an actual grip.

stands for its corresponding member's number. T_i and T_i' are equal in size and opposite in direction. The angular relations are also marked in black in Fig. 5(b), where θ_1, θ_3, θ_5, θ_7, θ_8, θ_{10}, θ_{12}, α, β are the angles between $T_3$and x_1, T_3 and x_2, T_5 and x_2, T_7 and x_3, T_8 and x_3, T_{10} and x_4, T_{12} and x_4, T_{12} and member number 13, F_N and member number 14, respectively. In the coordinate $\mathrm{x}_1o_1y_1$, the governing equations according to equilibrium of forces can be obtained

$$T_3 \times \sin\theta_1 = F \tag{9}$$

$$T_3 \times \cos\theta_1 = T_4. \tag{10}$$

From (9), we have

$$T_3 = \frac{F}{\sin\theta_1}. \tag{11}$$

Similarly, in coordinate $\mathrm{x}_2o_2y_2$, we have the following equations according to equilibrium of forces:

$$T_5 \times \sin\theta_5 + T_3 \times \sin\theta_3 = T_1 \tag{12}$$

$$T_5 \times \cos\theta_5 = T_3 \times \cos\theta_3. \tag{13}$$

By substituting (11) and (12) into (13), we have

$$T_5 = \frac{F \times \cos\theta_3}{\sin\theta_1 \times \cos\theta_5}. \tag{14}$$

In the same way, by using force equilibrium method in coordinates $\mathrm{x}_3o_3y_3$ and $\mathrm{x}_4o_4y_4$, respectively, we finally have the relationship between the fingertip force F and the force F_N

$$F_N = \frac{\sin\alpha \cdot l_{13}}{\sin\beta \cdot l_{14}} \cdot \frac{\cos\theta_3\cos\theta_7\cos\theta_{10}}{\sin\theta_1\cos\theta_5\sin(\theta_8-\theta_7)\sin(\theta_{12}-\theta_{10})} \cdot F \tag{15}$$

where l_{13} and l_{14} are the lengths of the two levers of the V-shaped connection. The angles $\theta_1, \theta_2, \ldots, \theta_{10}$, α, and β defined in Fig. 5(b) have been measured in the grip test and shown in Fig. 5(c). From the measurement, we have

$$\theta_1 \approx \theta_5 = 34.0^\circ$$
$$\theta_3 \approx 0^\circ$$
$$\theta_7 = 25.2^\circ$$
$$\theta_{10} = 6.9^\circ$$
$$\alpha = 49.4^\circ$$
$$\beta = 110.7^\circ$$
$$\theta_8 - \theta_7 = 50.0^\circ$$
$$\theta_{12} - \theta_{10} = 43.1^\circ$$

In the design of the V-shaped connection, the lengths of the two levers are

$$l_{13} = 35 \text{ mm}$$
$$l_{14} = 30 \text{ mm}.$$

By substituting the above angles and lengths into (15), we have

$$F = \frac{\sin\beta \cdot l_{14}}{\sin\alpha \cdot l_{13}} \cdot \frac{\sin\theta_1\cos\theta_5\sin(\theta_8-\theta_7)\sin(\theta_{12}-\theta_{10})}{\cos\theta_3\cos\theta_7\cos\theta_{10}} \cdot F_N$$
$$\approx 0.285 \times 91.7 \approx 26.1 \text{ (N)}. \tag{16}$$

Therefore, in theory, the grip strength increases altogether by

$$F_{Theor} = F_i \times 4 = 104.4 \text{ (N)}.$$

III. Analysis of the MR Actuator

The mass fraction of ferromagnetic particles in MRG determines MRG bearing's locking torque at settled magnetic fields. Higher particle fraction results in stronger particle chains and higher locking torque under magnetic fields. However, increased particle fraction can cause higher rotational resistance when no magnetic field is applied, leading to higher resistive force of the MR actuator. To identify the optimal particle content, torque, and force tests were performed on MR bearings and MR actuators with varying particle mass fractions of MRG. In the tests, magnetic field intensity was set to either zero (0 T) or a high level (0.5 T). Results [see Fig. 6(a)] indicated that the average resistive torques of MRG bearings and average resistive forces of MR actuator at both magnetic levels rose with increasing particle mass fractions. The MRG bearings with 50% and 40% particle mass fractions, respectively, exhibited the largest and second largest average torque differences. However, the MRG bearing with 50% particle mass fraction showed a rapid increase in resistive torque at zero magnetic level compared to those with 40% or less. At the same time, the resistive force (12 N) of MR actuator with 50% particle mass fraction is 44% higher than that of 40% particle mass fraction, which seriously hinders the movement of the finger exoskeleton. Conversely, MRG bearing with 40% particle mass fraction showed an optimal balance, with high locking torque at high magnetic levels and sufficiently low resistive torque at zero magnetic level. Accordingly, MR actuator with MRG of 40% particle mass fraction also showed acceptable resistive force at zero magnetic level.

To maximize magnetic field utilization, the coil is sleeved over the inner sleeve and positioned between the two bearings. This arrangement could concentrate the magnetic flux and forms circuits within the inner sleeve, MRG bearing, outer sleeve, and plain bearing. To verify this hypothesis, we simulated the magnetic flux density in the MR actuator under an applied coil current of 0.5 A using COMSOL Multiphysics, as shown in Fig. 6(b(i)). The simulation results demonstrate the concentration of magnetic flux and circuits within the sleeves and bearings. The circuits go straight across the MRG bearing, enabling effective utilization of the magnetic field. In this simulation, MRG with a 40% particle mass fraction was used. To enhance the reliability of the results, the B-H (magnetic flux density versus magnetic field strength) curve of the used MRG was measured using an MPMS3 magnetometer (Quantum Design Inc.) and is presented in Fig. S3. Additionally, four probes were utilized in the simulation to measure magnetic flux intensities at different locations and current intensities, as shown in Fig. 6(b(ii)). The magnetic field intensity at probe 2 is much higher than other 3

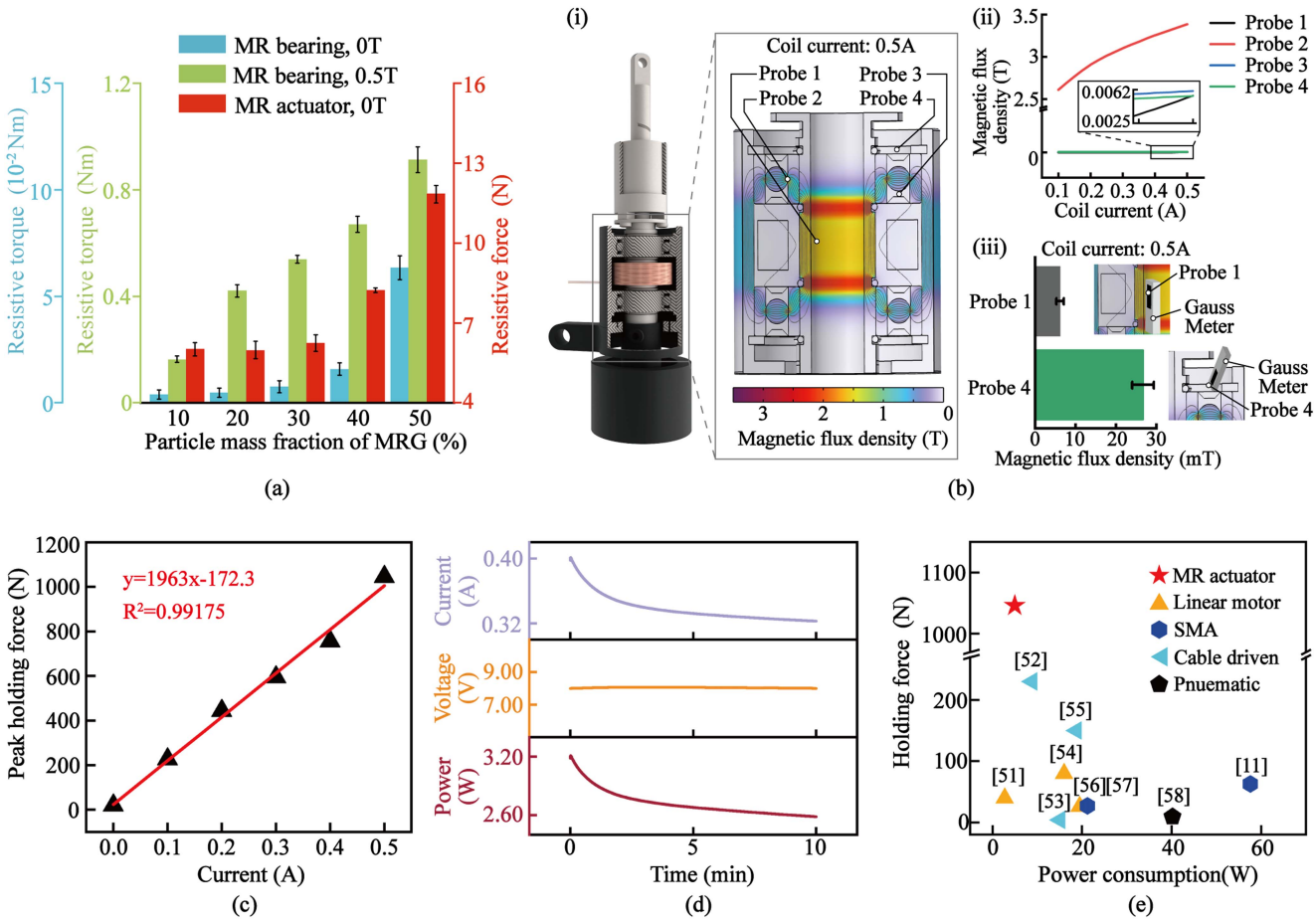

Fig. 6. Performance validation and electrical properties of the MR actuator. (a) Resistive torque and force of the MRG bearing and MR actuator, respectively, under varying particle mass fractions at zero (0 T) and high (0.5 T) magnetic field intensities. (b(i)) Magnetic field simulation of the MR actuator. (b(ii)) Oretical magnetic flux densities measured by the four probes shown in (b(i)) under varying current intensities. (b(iii)) Actual magnetic flux densities (average values, n = 8) measured by the Gauss meter at the locations of probes 1 and 4. (c) Peak holding force of the MR actuator at different coil current. (d) Electrical properties (current, voltage, and power consumption) of the MR actuator, exhibiting minimal variation during prolonged continuous operation. (e) Comparative analysis between the MR actuator and other actuators in some of the current researches regarding maximum holding force and energy consumption.

probes, showing a high concentration of magnetic flux within the MR bearing. To further examine the theoretical data, the actual magnetic flux intensities on the locations of probes 1 and 4 were measured using Gauss Meter with a coil current of 0.5 A. Each location was measured eight times, and the average values are shown in Fig. 6(b(iii)). The results demonstrate good agreement between the simulated and measured values at probe 1. However, a discrepancy was observed at probe 4, where the actual magnetic flux density was higher than the simulated value, indicating a limitation of the simulation model.

With the MRG bearing of optimal particle mass fraction of 40%, the performance of the MR actuator at different magnetic levels was then evaluated (Movie S1). Peak holding force of MR actuator is the most important for the MRHE, since it determines the MRHE's maximum grip support. The MR actuator was installed on a material test system (MTS, detailed illustration can be found in Fig. S4) for a linear tensile test and to obtain relationship between its holding force and coil's current, as shown in Fig. S5. In Fig. 6(c), the peak holding force has a positive correlation with coil current, with a wide adjustable range from several Newtons to over a thousand Newtons. At 0.5 A, the holding force peaks to 1046 N. The MR actuator's wide and easily controllable output force range provides advantages for its applications in MRHE and other robotic or intelligent mechanism designs.

Electrical characterization of the MR actuator powered by the control backpack was further tested. During a 10-min test, the current slightly decreased due to increased coil resistance caused by temperature rise, while the voltage remained almost stable [see Fig. 6(d)]. The current decrease is acceptable in rescue scenarios, as rescuers are unlikely to maintain a grip for as long as 10 minutes due to fatigue in other parts, such as arms, shoulders, and back. Breaks between tasks allow the coils to cool down, keeping the current drop minimal in practice. During the whole test, power consumption (current multiplied by voltage) remained between 3.2 W and 2.5 W.

A comparative analysis with conventional actuators used on hand exoskeletons [see Fig. 6(e)] revealed that the holding force of MR actuator is 4.55 times higher than the best (found in [52]) in the listed actuators (see detailed comparison in Table S1). Additionally, our work exhibited the highest force-to-power

ratio (209.2 N/W), outperforming the actuator in [52] by 7.95 times. Besides, the MR actuator reduces energy consumption by 97.7% compared to the actuator in [52], while producing the same holding force. The results demonstrate that the MR actuator surpasses the state-of-art in terms of holding force and power consumption, positioning it as a promising alternative for hand exoskeletons.

IV. Electrical Design and Control

For grip status analysis and control, fingertip pressure is measured using two piezoresistive pressure sensors located on the dorsal (sensor 1) and ventral (sensor 2) surfaces of the index fingertip, respectively, as shown in Fig. 2(a). The sensors' signals are processed by a sensor printed circuit board (PCB) and sent to the control backpack by a Bluetooth module, as depicted in Fig. 7(a). The PCBs are independently powered by a lithium battery. The control backpack in Fig. 7(b) consists of two sets of electrical components that work for left and right hand exoskeletons, respectively: STM32 microcontroller and Bluetooth module, lithium battery, digital-to-analog (DAC) converter and power amplifier. The micro controller and Bluetooth module receive sensor signals run the control algorithm. The batteries power the electrical components in the control backpack and the MRHE. The DAC converter converts digital signals from microcontroller into analog signals for the power amplifier, which enlarges the battery voltage for powering MR actuators.

The control methodology can be switched between grip strength enhancement and grip endurance enhancement based on user's intent [see Fig. 7(c)]. For grip strength enhancement, the MRHE is not powered, relying solely on harnessing human energy. For grip endurance enhancement, both sensors experience pressure during gripping, whereas only sensor 1 is under pressure during release. By evaluating sensor values, grip status can be classified, enabling automatic control of the hand exoskeleton based on user's intent.

To validate this method, the sensor values and output of control backpack were recorded during a grip-and-release period, as depicted in Fig. 7(d). Sensors 1 and 2 value rise synchronously above the setting threshold during gripping, while the control backpack powers the MRHE. Upon release, sensor 2 value decreases below the threshold first, followed by the power-down and demagnetization of the MRHE. In summary, this method enables simple yet effective control for the MRHE.

V. Experimental Results

All experiments were carried out in accordance with the declaration of Helsinki on research involving human subjects, and were approved by The First Affiliated Hospital of USTC (NO. 2023KY239). All subjects provided explicit written consent to participate in the study. Table I provides information about the subjects, including their gender, age, height, weight, and their professionalism in rescue. Additional details, such as the number of subjects and hand usage, are included in the descriptions of the subsequent experiments. For certain experiments, such as heavy lifting and casualty evacuation, multiple volunteers participated to show statistical differences between different subjects. While

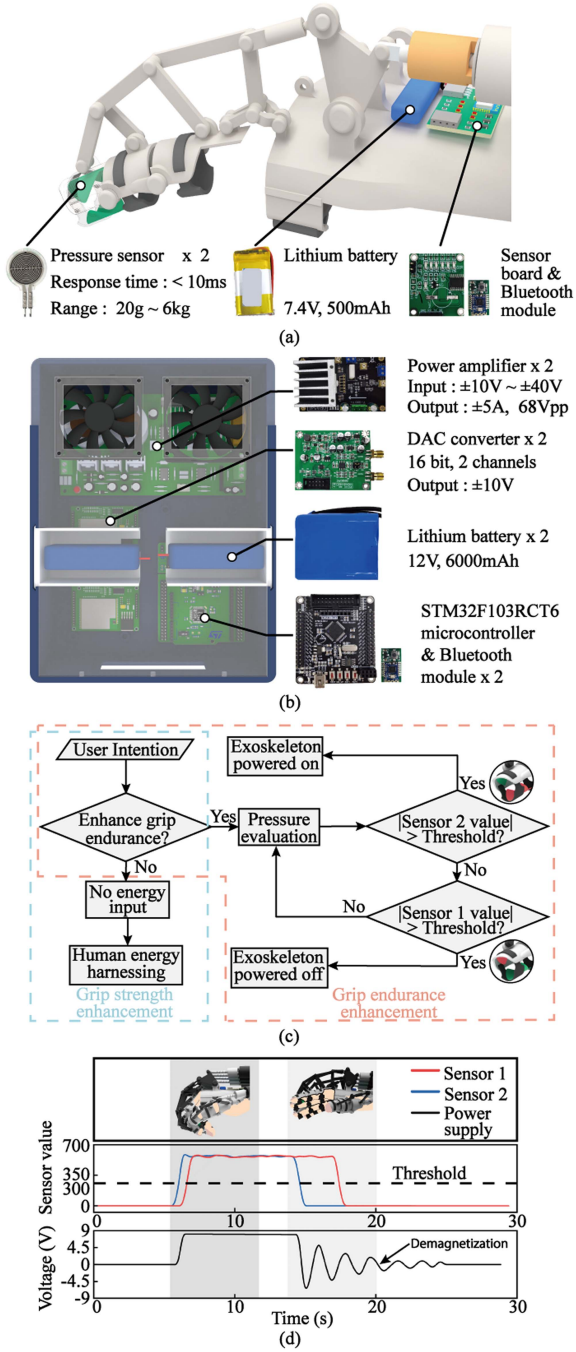

Fig. 7. Electronic design and overall control stratagem. (a) Overview of the pressure sensing hardware. (b) Overview of the control backpack's electronics hardware. (c) Control methodology regarding grip strength enhancement and grip endurance enhancement. (d) Correlation between pressure sensor value and control backpack output in a grip-and-release period.

TABLE I
Subject Information for the Experiments

	Gender	Age [years]	Height [cm]	Weight [kg]
Subject1	Male	25	176	83
Subject2	Male	23	170	76
Subject3	Male	19	183	66
Subject4	Male	21	185	80
Subject5	Male	24	185	88

IEEE Transactions on Robotics (T-RO) paper, presented at ICRA 2026, Vienna, Austria. Cite as T-RO paper.

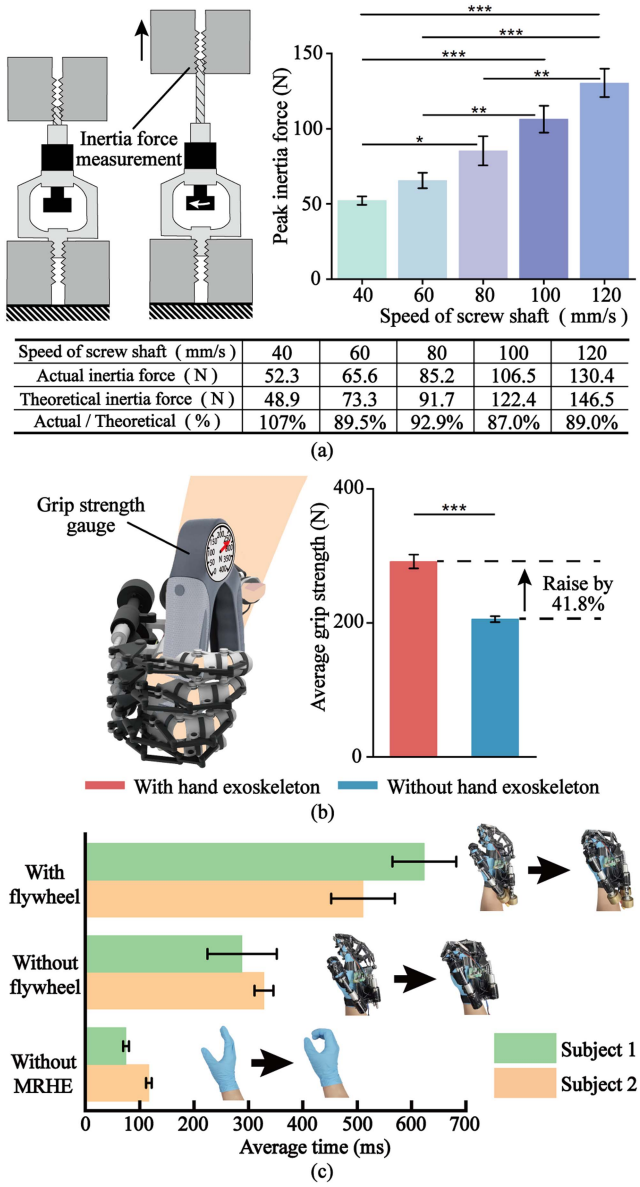

Speed of screw shaft (mm/s)	40	60	80	100	120
Actual inertia force (N)	52.3	65.6	85.2	106.5	130.4
Theoretical inertia force (N)	48.9	73.3	91.7	122.4	146.5
Actual / Theoretical (%)	107%	89.5%	92.9%	87.0%	89.0%

(a) (b) (c)

Fig. 8. Investigations on grip strength enhancement with MRHE. (a) Experimental setup and results of MR actuator in rapid tensile testing. Theoretical calculation is based on (8). (b) Grip strength testing with MRHE. Bars represent means. Error bars represent ±1 SD about the mean, and asterisks indicate statistical significance (multiple comparisons, $*P < 0.05$, $**P < 0.01$, $***P < 0.001$, n = 6). (c) Average gripping times under three conditions: MRHE with flywheels (off-state), MRHE without flywheels (OFF-state), and without MRHE. Error bars represent ±1 SD about the mean (n = 5).

for the dead hang challenge and postearthquake rescue, only Subject 1 demonstrated the experiments to focus on performance differences of the MRHE.

A. Grip Strength Enhancement

To validate the theoretical model, actual inertia force on the screw shaft was tested by using the MTS. The upper right portion of Fig. 8(a) illustrates the average peak inertia forces and their corresponding velocities (see detailed data in Table S2). The results show that as the speed increased, the generated peak inertia force increased simultaneously. This is because the ball screw first stored the driving energy in the rotating flywheel, and then converted the energy back to generate an inertia force on the screw shaft. This observation aligns with the design objectives that by harnessing human hand driving energy, it is effective to enhance grip strength without any external actuation. As shown in the table in Fig. 8(a), the actual peak inertia forces closely align with the theoretical values calculated using (8). The ratios of actual forces to theoretical forces are 107%, 89.5%, 92.9%, 87%, and 89%, respectively, with an average ratio of 93.08%. These results show the general accuracy of the model. However, due to the omission of rotational damping and energy dissipation of the MRG bearing, there will inevitably be deviations between the actual values and theoretical values.

In most hand exoskeleton designs, gripping motion is actively actuated to provide adequate grip strength for individuals with hand disabilities to perform daily activities. However, for ordinary people with intact hand functionality, the energy generated during gripping is sufficient to be harnessed to enhance grip strength. This is achievable by wearing the proposed MRHE according to the above performance validation of the MR actuator.

The impact of the proposed MR hand exoskeleton on grip strength enhancement was assessed with experiments (Movie S2). Only subject 1 participated in this experiment, using his right hand (handedness). The subject was instructed to complete six fast gripping actions without the MRHE, followed by six fast gripping actions with the MRHE. This is because the proposed design enhances grip strength only in fast gripping scenarios. To minimize the impact of the MRHE's range of motion on grip force, the gripping range under both conditions was kept as consistent as possible. Additionally, 20 s of rest were provided between each gripping action to allow for adjustments and recovery. Results in Fig. 8(b) show an increase of 85.8 N in mean grip strength with the MRHE, which is 41.8% higher than the condition without it. Considering the previous kinetic model of the MRHE, the experimental result is about 82.2% of the theoretical value F_{Theor}. This deviation may result from the frictions and efficiency in force transmission. Importantly, this augmentation in grip strength was achieved solely through the actuation and energy from the human hand, without any external energy consumption.

To evaluate the impact of the MRHE on finger movement in the OFF-state, the gripping process was recorded using a high-speed camera at 240 frames per second. The experiment involved two subjects (Subject 1 and 2) under three conditions: 1) MRHE with flywheels, 2) MRHE without flywheels, and 3) without MRHE. In each trial, subjects tried to apply consistent effort while gripping. As shown in Fig. 8(c), the average gripping time with the MRHE and flywheels significantly increased compared to the condition without MRHE. This is expected due to the increased total moment of inertia introduced by the flywheels, which poses a negative effect that should be addressed in future studies. However, when the goal is to enhance grip endurance, wearing the MRHE without the flywheels effectively reduces finger movement resistance. This is feasible since the flywheels are modular and can be easily detached from the MR

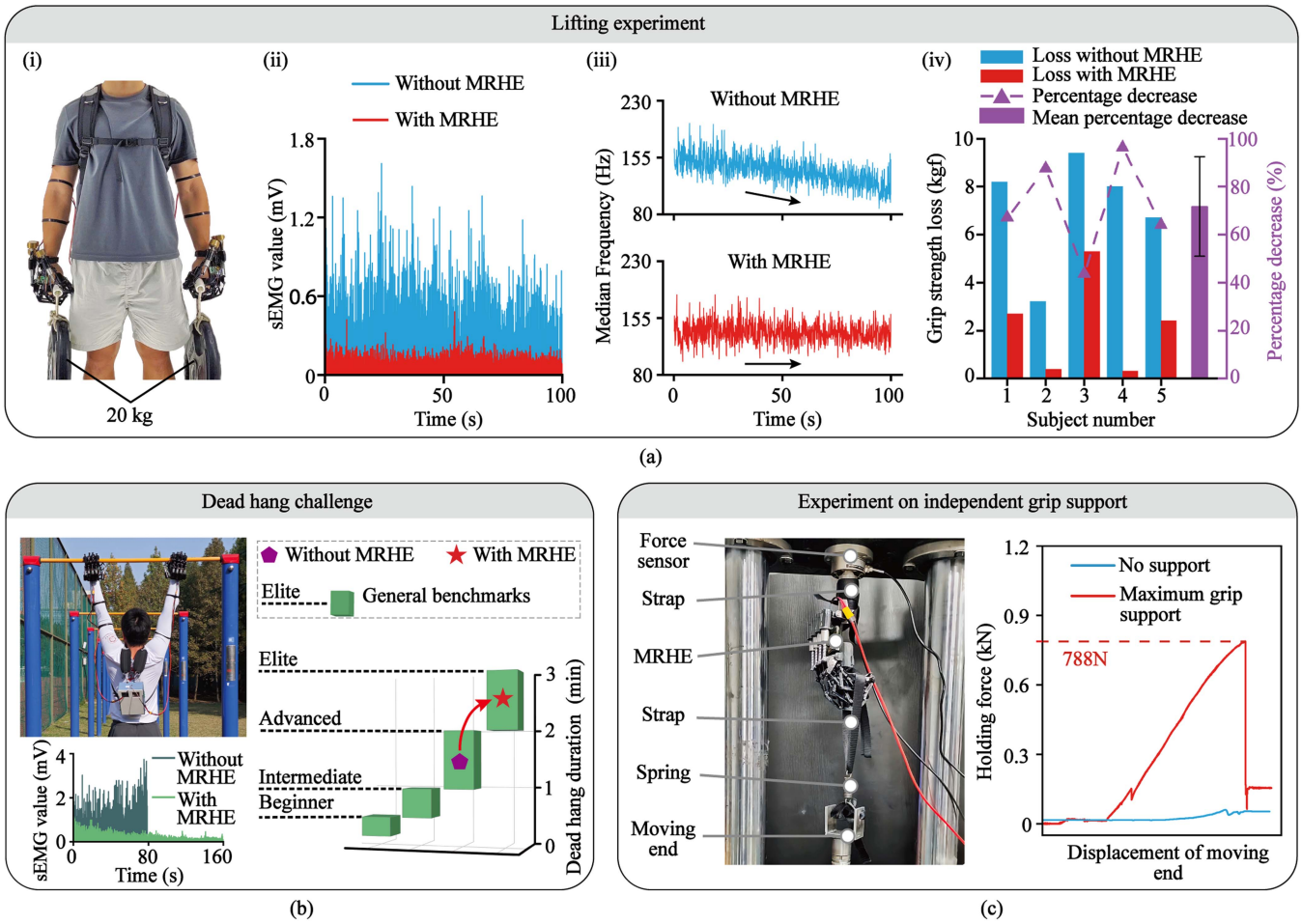

Fig. 9. Experiments on grip endurance enhancement with MRHE. (a) Experimental demonstration, sEMG values of flexor digitorum profundus, median frequencies of the sEMG data and grip strength loss data of the lifting experiment. Error bars represent ±1 SD about the mean. (b) Dead hang challenge to show the capacity to enhance human self-weight support of MRHE. (c) Experiment on assistance solely provided by the MRHE. The left figure illustrates the experimental setup on the MTS. The right figure depicts the relationship between holding force and the moving end's displacement under no-support (0 A overall supply current) and maximum-grip-support (2.5 A overall supply current) conditions, respectively.

actuators. In this scenario, the average gripping time for the two subjects decreased by 53.8% and 35.8%, respectively, as shown in Fig. 8(c).

B. Grip Endurance Enhancement

The MRHE's ability to enhance grip endurance and improve gripping capability was systematically investigated. Its performance in lifting heavy objects with wearing the MRHE system [see Fig. 9(a(i))] was first evaluated. During prolonged lifting of heavy loads, the hand exoskeletons bear most of the weight, reducing hand fatigue and enhancing grip endurance. To quantify this effect, surface electromyographic (sEMG) signals from the participant's forearm muscle (flexor digitorum profundus) were collected throughout the lifting experiments. The sEMG acquisition system and sensor placement can be found in Fig. S6 in Supplementary Materials. All sEMG data were processed in three steps: 1) selecting valid data segments, 2) applying a band-pass filter (100–400 Hz) to extract the relevant EMG frequency components, and 3) computing the absolute value of the filtered signal. The absolute sEMG value is one of the indicators of muscle contraction force. All five subjects listed in Table I participated using both hands. The sEMG data for Subject 2 are shown in Fig. 9(a(ii)) and Fig. 9(a(iii)) to illustrate the overall trend. Data for all subjects are provided in Fig. S7 in the Supplementary Materials. In Fig. 9(a(ii)), the sEMG value showed a significant reduction (red line) when the MR hand exoskeletons were worn by subject 2, indicating a noteworthy reduction in the participant's muscle contraction force. The sEMG signals of other four participants also showed the same trend, as detailed in Fig. S7.

From a longer-term perspective, the median frequency of sEMG signals illustrates participant's hand muscle fatigue. Muscle fatigue changes series of muscle biochemical reactions such as slowing down muscle fiber conduction and altering fiber recruitment, causing a decrease in sEMG median frequency. The experimental results [see Fig. 9(a(iii))] indicate that without hand exoskeletons, there is a consistent decrease in the median frequency of sEMG signals (blue curve), indicating a rapid onset of hand fatigue. In contrast, with the use of hand exoskeletons,

the median frequency of sEMG signals maintains relative stability (red curve), suggesting a notable reduction in hand fatigue.

In addition, hand fatigue can lead to a decrease in maximum grip strength. In the lifting experiments, the participants' maximum grip strengths were recorded both before and after the experiments to assess how the hand exoskeleton can mitigate their difference — the grip strength loss. Five participants were required to lift a load of 20 kg by each hand for 100 s both with and without wearing the MRHE system. Each participant first lifted the loads without the MRHE. After that, they relaxed for 30 min before lifting the loads with the MRHE. Each participant finished the test in a single day. Four of five participants experienced over 60% reduction in grip strength loss with wearing the MRHE system compared to not wearing it [see Fig. 9(a(iv))]. On average, the subjects experienced 71.7% reduction in grip strength loss. These results showed that hand fatigue was reduced by wearing the MRHE.

Having verified its ability in heavy lifting enhancement, the hand exoskeleton's capacity to enhance human self-weight support was further explored. There was one subject (subject 1) participated in the dead hang challenge (hanging from a bar with both hands for as long as possible) with and without the MRHE (Movie S3). There was a two-day rest period between the two experiments to allow the subject's hand muscles to recover from fatigue. Similarly, the sEMG signals of participant's forearm muscle and maximum endurance times were recorded. By comparing sEMG values during the experiments, it shows that less muscle contraction occurred when wearing the MRHE. For dead hang duration, typically, individuals without specialized training endure no more than 1 min [59], placing them at the "Beginner" or "Intermediate" level. Durations of 1 to 2 min and 2 to 3 min represent the "Advanced" and "Elite" levels, respectively. In the experiment, the participant endured only 1 min and 19 s with bare hands, being marked as "Advanced" level [see Fig. 9(b)]. While with the assistance of MRHE for his best effort, the maximum endurance time jumped to 2 min and 38 s, achieving the "Elite" level. Such improvement shows that MRHE can enhance the human self-weight support ability.

Following the human-centered experiments, the independent grip support assessment of the MRHE was conducted. As illustrated in Fig. 9(c), the MTS was used to apply an increasing force on the MRHE until it failed to sustain. One end of the MRHE was secured to a static tensile force sensor (DYLF-102, 0–100 kg, DAYSENSOR Co., Ltd.) using a strap, while the other end was pulled by the moving end of the MTS at a speed of 1 mm/s, also using a strap. Without powering the MR actuator for grip support, the MRHE's holding force remained below 34 N (blue line). When the MR actuators were powered, the measured force increased significantly (red line), peaking at 788 N before the hand exoskeleton failed to sustain. For comparison, the RoboGlove in [60] can generate a peak grasp force of approximately 222 N and a continuous grasp force ranging from 67 N to 89 N. The Space Suit RoboGlove in [61] can augment the test subjects' grasping force by about 45 N. The hand exoskeleton in [62] produces an average force of 30 N at each fingertip, but it only actuates two fingers to provide grip support. These comparisons demonstrate the substantial grip support capabilities of the MRHE.

C. Applications of the MR Hand Exoskeletons

Despite advancements in large-scale tools designed to replace human labor, human-led operations remain more effective and practical, especially in postearthquake scenarios where human rescuers are pivotal. The following experiments were conducted only on subject 1 with both hands over several days in separate sessions. In Fig. 10(a), the simulation depicts an artificial man trapped under a large stone slab. Without the exoskeleton, the subject lacked sufficient grip strength to move the stone and rescue the survivor (Movie S4). Conversely, with the exoskeleton, lifting became manageable, and the sEMG signal amplitudes revealed a notable reduction in hand muscle exertion compared to efforts without the exoskeleton.

The hand exoskeletons also demonstrated their performance in continuous rescue operations and debris clearance [see Fig. 10(b)]. The participant continuously turned up five stone slabs of the same weight (Movie S5). The forearm sEMG signals shown that muscle exertion time decreased during such continuous use by wearing MRHE. Then, the integrated EMG (iEMG) data for the contrast experiments was calculated. The iEMG with MRHE decreased by 52%, indicating a much lower muscle contraction in this condition. However, in these two rescue experiments, the effort from bigger muscle groups cannot be ignored, such as those in the upper and lower body. This represents the limitations of these assessments.

Additionally, casualty evacuation scenario was simulated by carrying a 60 kg artificial man with a stretcher on a treadmill at the speed of 3 km/h [see Fig. 10(c)]. This experiment was conducted by all five subjects for repeated evaluation. And subject 1 was asked to do repeated tests to gather data on heart rate, respiration rate, and maximum endurable distance in a single day, with a 30-min rest between each test. Similarly, sEMG graph showed less muscle contraction when wearing the MRHE. The participant's heart rate and respiratory rate during the tests were also measured using a heart rate belt for further evaluation. When wearing the MRHE, the participant's average heart rate was slightly lower than not wearing the MRHE (decreased by 1.2%). The respiratory rates showed notable difference. The participant's average respiratory rate with MRHE decreased by 20% compared to not wearing it, indicating less oxygen consumption and a lower metabolic rate (same depth of respiratory was controlled at any experimental conditions). In addition, the participant with MRHE carried the stretcher much longer (110% longer time) than with bare hands. It should be noted that it was aches from the shoulder and back muscles that limited the participant from carrying longer with MRHE, rather than muscles of hand and arm.

Additionally, applications such as horizontal ladder climbing, vertical ladder climbing, and rock climbing were tested (Movies S6 to S8) and showed the MRHE's potential in finishing these works.

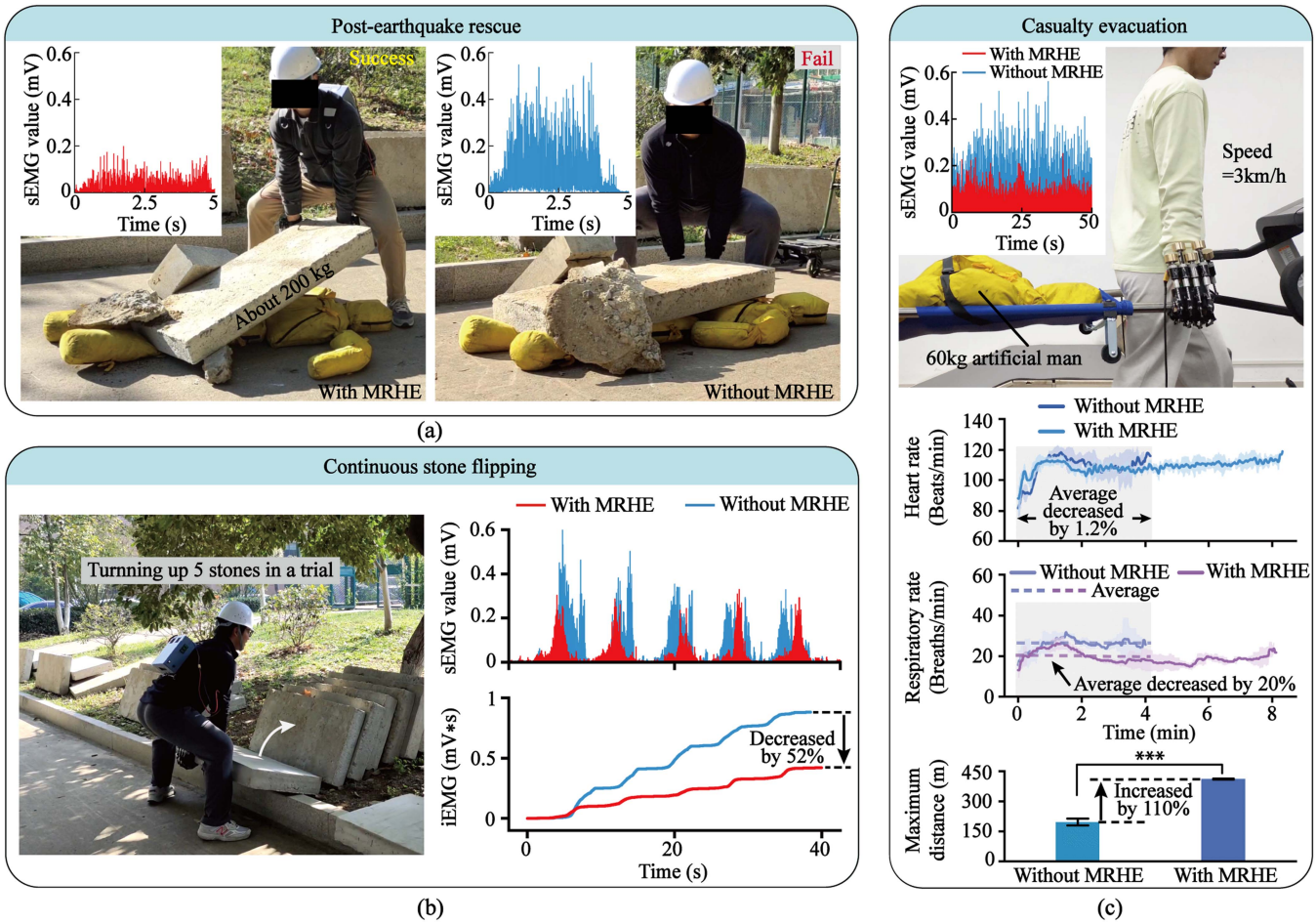

Fig. 10. Application scenarios and effects of the MRHE. (a) Postearthquake rescue simulation. An artificial man was trapped under a large stone of about 200 kg. The participant tried to remove the stone away with and without the help of MRHE. (b) Continuous stone flipping to simulate continuous postearthquake rescue and clearance operations. (c) Casualty evacuation simulation with stretcher on a treadmill. Heart rate, respiratory rate and maximum distance during the tests are recorded and compared. Bars represent means. Error bars represent ± 1 SD about the mean, and asterisks indicate statistical significance (multiple comparisons, $*P < 0.05$, $**P < 0.01$, $***P < 0.001$, $n = 5$).

VI. Conclusion

This work presents a nonmotorized MR hand exoskeleton that substantially elevates user's grip strength and endurance. These functions can prominently help rescuers release hand fatigue and improve working efficiency. To achieve these functions, we developed an MR actuator capable of harnessing human energy for grip strength enhancement, while also offering a high supporting force for gripping augmentation and grip endurance enhancement. Contrary to actively driven hand exoskeletons designed for disabled individuals, the semiactive MRHE offers a high force-to-power ratio for healthy users. Such performance stems from the novel energy-harvesting architecture and utilization of MR technology features—high force, fast response, and energy-efficient.

The MR actuator and other hand exoskeleton actuators were compared in terms of holding force and power consumption, where the MR actuator outperforms others in both aspects. Previous hand exoskeletons were mainly designed for the elderly or disabled, achieving actively-controlled finger motion range and sufficient force for daily activities [51], [53], [54], [55], [57], [58]. However, for healthy individuals in high-load-capacity scenarios, such active actuation is unnecessary and inadequate to provide high supporting force. In contrast, the MR actuator demonstrates a power-to-volume ratio one-order-of-magnitude higher than conventional approaches.

Series of experiments were conducted to assess the enhancement of grip strength and endurance by MR actuators and hand exoskeletons. The MTS was first employed to independently simulate the rapid activation of the MR actuator by a finger. Experimental results showed a trend of positive correlation between the driving speed and the generated inertia force. Then, grip strengths with and without wearing the hand exoskeleton were measured using a dynamometer, showing an average increase of 41.8% when the MRHE was worn. These results validate the efficacy of the MR hand exoskeleton in significantly enhancing grip strength.

Although the optimal magnetic particle ratio has been identified, we acknowledge that the proposed mechanism inherently introduces some resistance to finger movement compared to

barehanded operation. This resistance has slight negative impact on finger dexterity and speed. However, such effect is not a problem for hand manipulation considering the powerful assistance the MRHE system provides. And this tradeoff is a common challenge faced by most assistive exoskeleton systems.

The MR actuator's holding force was also systematically evaluated using the MTS. The MR actuator had a wide span of peak holding force, ranging from several Newtons to over a thousand Newtons. According to the results, the MR actuator can generate a peak holding force of 1046 N with coil current of 0.5 A, surpassing traditional actuators of the same size. We then investigated how the MR hand exoskeletons enhance grip endurance. In the lifting test, wearing the MRHE significantly reduced hand muscle activity and fatigue. Four of five participants experienced over 60% reduction in grip strength loss compared to not wearing the exoskeletons. In the dead hang challenge, the participant doubled their endurance time and jumped from "Advanced" level to "Elite" level with the assistance of MRHE. Additionally, without being wore by human hand, the MRHE can provide holding force up to 788 N independently. These results underscore the MR hand exoskeleton's capacity to enhance grip endurance.

Furthermore, various real-world scenarios to test the MR hand exoskeletons' practical use were simulated. Whether in post-earthquake survivor rescue, debris clearance, or casualty evacuation, the exoskeletons showed competent in reducing wearers' hand fatigue, lowering metabolic rate, and concurrently enhancing operational efficiency.

In practical implementation, the proposed design does have some limitations. First, the MR hand exoskeletons are slightly heavy for prolonged usage. Specifically, one hand exoskeleton weighs 1.7 kg, with approximately 1.2 kg attributed to five MR actuators, primarily from the flywheel. The necessity of ferromagnetic materials, like low carbon steel, for constructing magnetic paths for MR bearings also contributes to this weight. Second, the optimization in structural design is imperative to enhance the exoskeleton's motion range and force transmission efficiency. Current motion range constraints may hinder genuine augmentation of user grip strength. Additionally, more precise kinematic modeling is necessary to align the exoskeleton with natural hand movement, minimizing force dissipation for better performance. Addressing these limitations through future refinement will optimize the practicality of the MR hand exoskeleton design.

REFERENCES

[1] M. R. Cutkosky, "On grasp choice, grasp models, and the design of hands for manufacturing tasks," *IEEE Trans. Robot. Automat.*, vol. 5, no. 3, pp. 269–279, Jun. 1989, doi: 10.1109/70.34763.

[2] T. Shahid, D. Gouwanda, S. G. Nurzaman, and A. A. Gopalai, "Moving toward soft robotics: A decade review of the design of hand exoskeletons," *Biomimetics*, vol. 3, no. 3, 2018, Art. no. 17, doi: 10.3390/biomimetics3030017.

[3] S. R. Soekadar et al., "Hybrid EEG/EOG-based brain/neural hand exoskeleton restores fully independent daily living activities after quadriplegia," *Sci. Robot.*, vol. 1, 2016, Art. no. eaag3296, doi: 10.1126/scirobotics.aag3296.

[4] P. E. Dupont et al., "A decade retrospective of medical robotics research from 2010 to 2020," *Sci. Robot.*, vol. 6, 2021, Art. no. eabi8017, doi: 10.1126/scirobotics.abi8017.

[5] P. Heo, G. Gu, S. Lee, K. Rhee, and J. Kim, "Current hand exoskeleton technologies for rehabilitation and assistive engineering," *Int. J. Precis. Eng. Manuf.*, vol. 13, pp. 807–824, 2012, doi: 10.1007/s12541-012-0107-2.

[6] M. Sarac, M. Solazzi, and A. Frisoli, "Design requirements of generic hand exoskeletons and survey of hand exoskeletons for rehabilitation, assistive, or haptic use," *IEEE Trans. Haptics*, vol. 12, no. 4, pp. 400–413, Oct.–Dec. 2019, doi: 10.1109/TOH.2019.2924881.

[7] P. Ben-Tzvi and Z. Ma, "Sensing and force-feedback exoskeleton (SAFE) robotic glove," *IEEE Trans. Neural Syst. Rehabil. Eng.*, vol. 23, no. 6, pp. 992–1002, Nov. 2015, doi: 10.1109/TNSRE.2014.2378171.

[8] M. B. Hong, S. J. Kim, Y. S. Ihn, G.-C. Jeong, and K. Kim, "KULEX-hand: An underactuated wearable hand for grasping power assistance," *IEEE Trans. Robot.*, vol. 35, no. 2, pp. 420–432, Apr. 2019, doi: 10.1109/TRO.2018.2880121.

[9] F. Chinello, M. Malvezzi, D. Prattichizzo, and C. Pacchierotti, "A modular wearable finger interface for cutaneous and kinesthetic interaction: Control and evaluation," *IEEE Trans. Ind. Electron.*, vol. 67, no. 1, pp. 706–716, Jan. 2020, doi: 10.1109/TIE.2019.2899551.

[10] H. K. Yap, N. Kamaldin, J. H. Lim, F. A. Nasrallah, J. C. H. Goh, and C. -H. Yeow, "A magnetic resonance compatible soft wearable robotic glove for hand rehabilitation and brain imaging," *IEEE Trans. Neural Syst. Rehabil. Eng.*, vol. 25, no. 6, pp. 782–793, Jun. 2017, doi: 10.1109/TNSRE.2016.2602941.

[11] Á. Villoslada, C. Rivera, N. Escudero, F. Martín, D. Blanco, and L. Moreno, "Hand exo-muscular system for assisting astronauts during extravehicular activities," *Soft Robot.*, vol. 1, pp. 21–37, 2019, doi: 10.1089/soro.2018.0020.

[12] M. Sreekumar, T. Nagarajan, M. Singaperumal, M. Zoppi, and R. Molfino, "Critical review of current trends in shape memory alloy actuators for intelligent robots," *Ind. Robot*, vol. 34, no. 4, pp. 285–294, 2007, doi: 10.1108/01439910710749609.

[13] S. Zaidi, M. Maselli, C. Laschi, and C. Matteo, "Actuation technologies for soft robot grippers, and manipulators: A review," *Curr. Robot. Rep.*, vol. 2, pp. 355–369, 2021, doi: 10.1007/s43154-021-00054-5.

[14] R. Morales, F. J. Badesa, N. García-Aracil, M. S. José, and P. Carlos, "Pneumatic robotic systems for upper limb rehabilitation," *Med. Biol. Eng. Comput.*, vol. 49, pp. 1145–1156, 2011, doi: 10.1007/s11517-011-0814-3.

[15] D. Bruder, M. A. Graule, C. B. Teeple, and R. J. Wood, "Increasing the payload capacity of soft robot arms by localized stiffening," *Sci. Robot.*, vol. 8, 2023, Art. no. eadf9001, doi: 10.1126/scirobotics.adf9001.

[16] M. Wehner et al., "Pneumatic energy sources for autonomous and wearable soft robotics," *Soft Robot.*, vol. 1, pp. 263–274, 2014, doi: 10.1089/soro.2014.0018.

[17] N. S. K. Ho et al., "An EMG-driven exoskeleton hand robotic training device on chronic stroke participants: Task training system for stroke rehabilitation," in *Proc. IEEE Int. Conf. Rehabil. Robot.*, 2011, pp. 1–5, doi: 10.1109/ICORR.2011.5975340.

[18] I. Jo and J. Bae, "Design and control of a wearable and force-controllable hand exoskeleton system," *Mechatronics*, vol. 41, pp. 90–101, 2017, doi: 10.1016/j.mechatronics.2016.12.001.

[19] M. Dragusanu, M. Z. Iqbal, T. L. Baldi, D. Prattichizzo, and M. Malvezzi, "Design, development, and control of a hand/wrist exoskeleton for rehabilitation and training," *IEEE Trans. Robot.*, vol. 38, no. 3, pp. 1472–1488, Jun. 2022, doi: 10.1109/TRO.2022.3172510.

[20] T. Bützer, O. Lambercy, J. Arata, and R. Gassert, "Fully wearable actuated soft exoskeleton for grasping assistance in everyday activities," *Soft Robot.*, vol. 8, pp. 128–143, 2021, doi: 10.1089/soro.2019.0135.

[21] M. Cempini, M. Cortese, and N. Vitiello, "A powered finger–Thumb wearable hand exoskeleton with self-aligning joint axes," *IEEE/ASME Trans. Mechatron.*, vol. 20, no. 2, pp. 705–716, Apr. 2015, doi: 10.1109/TMECH.2014.2315528.

[22] B. W. Gasser, D. A. Bennett, C. M. Durrough, and M. Goldfarb, "Design and preliminary assessment of Vanderbilt hand exoskeleton," in *Proc. Int. Conf. Rehabil. Robot.*, 2017, pp. 1537–1542, doi: 10.1109/ICORR.2017.8009466.

[23] M. Laffranchi et al., "The Hannes hand prosthesis replicates the key biological properties of the human hand," *Sci. Robot.*, vol. 5, 2020, Art. no. eabb0467, doi: 10.1126/scirobotics.abb0467.

[24] P. Kieliba, D. Clode, R. O. Maimon-Mor, and T. R. Makin, "Robotic hand augmentation drives changes in neural body representation," *Sci. Robot.*, vol. 6, 2021, Art. no. eabd7935, doi: 10.1126/scirobotics.abd7935.

[25] S. Diller, C. Majidi, and S. H. Collins, "A lightweight, low-power electroadhesive clutch and spring for exoskeleton actuation," in *Proc. IEEE Int. Conf. Robot. Automat.*, 2016, pp. 682–689, doi: 10.1109/ICRA.2016.7487194.

[26] D. Lee, H. Yu, and J. Bae, "Development of a soft semi-active suit using electro-static clutches for assisting static holding tasks," *IEEE Robot. Automat. Lett.*, vol. 9, no. 3, pp. 2814–2821, Mar. 2024, doi: 10.1109/LRA.2024.3360808.

[27] D. Wei et al., "Electrostatic adhesion clutch with superhigh force density achieved by MXene-poly(Vinylidene Fluoride–Trifluoroethylene–Chlorotrifluoroethylene) composites," *Soft Robot.*, vol. 10, no. 3, pp. 482–492, 2023, doi: 10.1089/soro.2022.0013.

[28] A. J. Carey and S. Robinson, "An unpowered exoskeleton to reduce astronaut hand fatigue during microgravity EVA," in *Proc. AIAA Space*, 2016, doi: 10.2514/6.2016-5390.

[29] E. M. Refour, B. Sebastian, R. J. Chauhan, and P. Ben-Tzvi, "A general purpose robotic hand exoskeleton with series elastic actuation," *J. Mechanisms Robot.*, vol. 11, 2019, Art. no. 060902, doi: 10.1115/1.4044543.

[30] E. R. Triolo, M. H. Stella, and B. F. BuSha, "A force augmenting exoskeleton for the human hand designed for pinching and grasping," in *Proc. 40th Annu. Int. Conf. IEEE Eng. Med. Biol. Soc.*, 2018, pp. 1875–1878, doi: 10.1109/EMBC.2018.8512606.

[31] J. Yang et al., "Equipping new SMA artificial muscles with controllable MRF exoskeletons for robotic manipulators and grippers," *IEEE/ASME Trans. Mechatron.*, vol. 27, no. 6, pp. 4585–4596, Dec. 2022, doi: 10.1109/TMECH.2022.3157329.

[32] J. Dai, H. Chang, R. Zhao, J. Huang, K. Li, and S. Xie, "Investigation of the relationship among the microstructure, rheological properties of MR grease and the speed reduction performance of a rotary micro-brake," *Mech. Syst. Signal Process.*, vol. 116, pp. 741–750, 2019, doi: 10.1016/j.ymssp.2018.07.004.

[33] A. Yi, A. Zahedi, Y. Wang, U. -X. Tan, and D. Zhang, "A novel exoskeleton system based on magnetorheological fluid for tremor suppression of wrist joints," in *Proc. IEEE 16th Int. Conf. Rehabil. Robot.*, 2019, pp. 1115–1120, doi: 10.1109/ICORR.2019.8779363.

[34] A. Zahedi, B. Zhang, A. Yi, and D. Zhang, "A soft exoskeleton for tremor suppression equipped with flexible semiactive actuator," *Soft Robot.*, vol. 8, pp. 432–447, 2021, doi: 10.1089/soro.2019.0194.

[35] M. R. Jolly, J. D. Carlson, and B. C. Muñoz, "A model of the behaviour of magnetorheological materials," *Smart Mater. Structures*, vol. 5, pp. 607–614, 1996, doi: 10.1088/0964-1726/5/5/009.

[36] G. Liu, F. Gao, D. Wang, and W. Liao, "Medical applications of magnetorheological fluid: A systematic review," *Smart Mater. Structures*, vol. 31, 2022, Art. no. 043002, doi: 10.1088/1361-665X/ac54e7.

[37] R. M. A. Dutra, R. M. de Andrade, A. B. Soares, N. V. Thakor, and C. B. S. Vimieiro, "Magnetorheological fluid in prostheses: A state-of-the-art review," *J. Intell. Mater. Syst. Structures*, vol. 35, no. 5, pp. 485–516, doi: 10.1177/1045389X231213126.

[38] J. Fu, J. Bai, J. Lai, P. Li, M. Yu, and H.-K. Lam, "Adaptive fuzzy control of a magnetorheological elastomer vibration isolation system with time-varying sinusoidal excitations," *J. Sound Vib.*, vol. 456, pp. 386–406, 2019, doi: 10.1016/j.jsv.2019.05.046.

[39] L. Ding et al., "Ultrasensitive multifunctional magnetoresistive strain sensor based on hair-like magnetization-induced pillar forests," *Adv. Electron. Mater.*, vol. 6, 2019, Art. no. 1900653, doi: 10.1002/aelm.201900653.

[40] T. Togawa, T. Tachibana, Y. Tanaka, and J. Peng, "Hydrodisk-type of electrorheological brakes for small mobile robots," *Int. J. Hydromechatron.*, vol. 4, pp. 99–115, 2021, doi: 10.1504/IJHM.2021.116955.

[41] S. A. Abdul Aziz, S. A. Mazlan, N. I. Nik Ismail, S.-B. Choi, Ubaidillah, and N. A. B. Yunus, "An enhancement of mechanical and rheological properties of magnetorheological elastomer with multiwall carbon nanotubes," *J. Intell. Mater. Syst. Structures*, vol. 28, pp. 3127–3138, 2017, doi: 10.1177/1045389X17705211.

[42] T. Hu, S. Xuan, L. Ding, and X. Gong, "Stretchable and magneto-sensitive strain sensor based on silver nanowire-polyurethane sponge enhanced magnetorheological elastomer," *Mater. Des.*, vol. 156, pp. 528–537, 2018, doi: 10.1016/j.matdes.2018.07.024.

[43] J. M. Ginder, "Behavior of magnetorheological fluids," *MRS Bull.*, vol. 23, pp. 26–29, 1998, doi: 10.1557/S0883769400030785.

[44] N. Mohamad and S. A. Mazlan, and Ubaidillah, "Effect of carbonyl iron particles composition on the physical characteristics of MR grease," *AIP Conf. Proc.*, vol. 1717, 2016, Art. no. 040027, doi: 10.1063/1.4943470.

[45] M. H. Ahmad Khairi et al, "Role of additives in enhancing the rheological properties of magnetorheological solids: A review," *Adv. Eng. Mater.*, vol. 21, 2019, Art. no. 1800696, doi: 10.1002/adem.201800696.

[46] B. J. Makinson, "Research and development prototype for Ma chine augmentation of Human strength and endurance. Hardiman I Project," General Electric Report S-71-1056, Schenectady, NY, USA, May 1971.

[47] Army-Technology, "Raytheon XOS 2 Exoskeleton, second-generation robotics suit - Army technology," 2015. [Online]. Available: http://www.army-technology.com/projects/raytheon-xos-2-exoskeleton-us/

[48] M. Fontana, R. Vertechy, S. Marcheschi, F. Salsedo, and M. Bergamasco, "The body extender: A full-body exoskeleton for the transport and handling of heavy loads," *IEEE Robot. Automat. Mag.*, vol. 21, no. 4, pp. 34–44, Dec. 2014, doi: 10.1109/MRA.2014.2360287.

[49] T. J. Armstrong, J. A. Foulke, B. J. Martin, J. Gerson, and D. M. Rempel, "Investigation of applied forces in alphanumeric keyboard work," *Amer. Ind. Hyg. Assoc. J.*, vol. 55, no. 1, pp. 30–35, 1994, doi: 10.1080/15428119491019230.

[50] J. Dennerlein Jr., C. Mote, and D. Rempel, "Control strategies for finger movement during touch-typing the role of the extrinsic muscles during a keystroke," *Exp. Brain Res.*, vol. 121, pp. 1–6, 1998, doi: 10.1007/s002210050430.

[51] C. J. Nycz, T. Bützer, O. Lambercy, J. Arata, G. S. Fischer, and R. Gassert, "Design and characterization of a lightweight and fully portable remote actuation system for use with a hand exoskeleton," *IEEE Robot. Automat. Lett.*, vol. 1, no. 2, pp. 976–983, Jul. 2016, doi: 10.1109/LRA.2016.2528296.

[52] J. Dittli, U. A. T. Hofmann, T. Bützer, G. Smit, O. Lambercy, and R. Gassert, "Remote actuation systems for fully wearable assistive devices: Requirements, selection, and optimization for out-of-the-lab application of a hand exoskeleton," *Front. Robot. AI*, vol. 7, 2021, Art. no. 596185, doi: 10.3389/frobt.2020.596185.

[53] D. Marconi, A. Baldoni, Z. McKinney, M. Cempini, S. Crea, and N. Vitiello, "A novel hand exoskeleton with series elastic actuation for modulated torque transfer," *Mechatronics*, vol. 61, pp. 69–82, 2019, doi: 10.1016/j.mechatronics.2019.06.001.

[54] W Chen et al., "Soft exoskeleton with fully actuated thumb movements for grasping assistance," *IEEE Trans. Robot.*, vol. 38, no. 4, pp. 2194–2207, Aug. 2022, doi: 10.1109/TRO.2022.3148909.

[55] U. A. T. Hofmann, T. Bützer, O. Lambercy, and R. Gassert, "Design and evaluation of a Bowden-cable-based remote actuation system for wearable robotics," *IEEE Robot. Automat. Lett.*, vol. 3, no. 3, pp. 2101–2108, Jul. 2018, doi: 10.1109/LRA.2018.2809625.

[56] B. P. Ruddy, "High force density linear permanent magnet motors: 'electromagnetic muscle actuators,'" Ph.D. dissertation, Massachusetts Institute of Technology, Cambridge, MA, USA, 2012.

[57] T. Tang, D. Zhang, T. Xie, and X. Zhu, "An exoskeleton system for hand rehabilitation driven by shape memory alloy," in *Proc. IEEE Int. Conf. Robot. Biomimetics*, 2013, pp. 756–761, doi: 10.1109/ROBIO.2013.6739553.

[58] O. Ramos, M. Múnera, M. Moazen, H. Wurdemann, and C. A. Cifuentes, "Assessment of soft actuators for hand exoskeletons: Pleated textile actuators and Fiber-reinforced silicone actuators," *Front. Bioeng. Biotechnol.*, vol. 10, 2022, Art. no. 924888, doi: 10.3389/fbioe.2022.924888.

[59] R. Turp, "Dead hang time Chart," 2023. [Online]. Available: https://fitnessdrum.com/dead-hang-time-chart/

[60] M. A. Diftler et al., "RoboGlove—A grasp assist device for Earth and Space," in *Proc. 45th Int. Conf. Environ. Syst.*, 2015. [Online]. Available: https://ntrs.nasa.gov/citations/20150010420

[61] J. M. Rogers, B. J. Peters, E. A. Laske, and E. R. McBryan, "Development and testing of robotically assisted extravehicular activity gloves," in *Proc. 47th Int. Conf. Environ. Syst.*, 2017, pp. 1–14. [Online]. Available: https://ntrs.nasa.gov/citations/20160013660

[62] E. K. Jian, D. Gouwanda Chan, and T. Kok Kheng, "Wearable hand exoskeleton for activities of daily living," in *Proc. IEEE-EMBS Conf. Biomed. Eng. Sci.*, 2018, pp. 221–225, doi: 10.1109/IECBES.2018.8626719.

Xianlong Mai received the B.Sc. degree in theoretical and applied mechanics in 2021 from the University of Science and Technology of China, Hefei, China, where he is currently working toward the Ph.D. degree in instruments science and technology.

His research interests include wearable exoskeleton, human-robot interaction, and robot teleoperation.

Jian Yang received the Ph.D. degree in mechatronics from the University of Wollongong, Wollongong, NSW, Australia, in 2017.

Then, she was employed as a Postdoctoral Research Fellow with the University of Wollongong from 2017. Later she was granted as the Research Fellow of Japan Society for Promotion of Science with Tohoku University, Japan, from 2019 to 2020. She is currently with Anhui University, Hefei, China. She has so far authored or coauthored more 30 papers published in top journals including MSSP, SMA, and JIMSS with 713 citations. Her research interests include vibration control, magnetorheological technology, and mechatronic systems

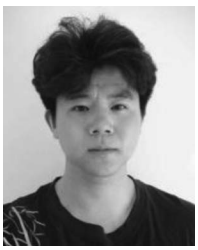

Lei Li received the B.S. degree in mechanical design and manufacturing in 2022 from the University of Science and Technology of China, Hefei, China, where he is currently working toward the Ph.D. degree in planetary science and exploration technology.

His research interests include wearable upper limb exoskeletons, large-burst magnetorheological driven joints, and high-performance mobile detection platforms.

Bin Zi received the Ph.D. degree in mechatronic engineering from Xidian University, Xi'an, China, in 2007.

He was a Visiting Scholar with the Chair of Mechanics and Robotics, University of Duisburg Essen, Germany, from 2011 to 2012, and a Visiting Professor with the Robotics and Automation Laboratory, Institute of Technology, University of Ontario, Canada, in 2015. He is currently the Dean and a Full Professor with the School of Mechanical Engi neering and the Director with the Robotics Institute, Hefei University of Technology, China. His research interests include the theory, technology, and equipment of rigid-flexible cou pling intelligent robots, control and automation of intelligent manufacturing systems, and multirobot systems.

Shiwu Zhang (Member, IEEE) received the B.S. degree in mechanical and electrical engineering and the Ph.D. degree in precision instrumentation and precision machinery from the University of Science and Technology of China (USTC), Hefei, China, in 1997 and 2003, respectively.

He is currently a Professor with the Department of Precision Machinery and Precision Instrumentation, USTC. He has authored or coauthored more than 100 journal and conference papers.

Xinglong Gong received the Ph.D. degree in mechanics from the University of Science and Technology of China (USTC), Hefei, China, and from Saitama University, Saitama, Japan, in 1996.

He is currently a Professor with the School of Engineering Science, USTC, Hefei, China. Then, he was with the Nihon Dempa Kogyo Co., Ltd., Japan, for seven years, as an Engineer and then a Chief Engineer. In 2003, he was with the Department of Modern Mechanics, USTC, as a Full Professor. His research interests include the soft matter materials including magnetorheological materials, shear thickening materials, polymer nanocomposites, as well as their application in the vibration isolator, vibration absorber, antishock equipment, and body armor.

Weihua Li received the Ph.D. degree in mechanical engineering from Nanyang Technological University, Singapore, in 2001.

He is a Senior Professor and Academic Program director for Mechatronic Engineering with the University of Wollongong. He was Specialty Chief Editor for Frontiers in Materials and Associate Editor or Editorial Board Member for other ten international journals, including Smart Materials and Structures, Lab on a Chip, IEEE/ASME TRANSACTIONS ON MECHATRONICS. As the General Chair, he organized two international conferences. He has authored and coauthored more than 350 journal papers with an h-index of 91 (Google Scholar).

Guolin Yun received the B.S. degree in theoretical and applied mechanics from the University of Science and Technology of China, Hefei, China, in 2017, and the Ph.D. degree in mechanical engineering from the University of Wollongong, Wollongong, NSW, Australia, in 2021.

He was the Royal Society Newton International Fellow and Senior Research Associate with the University of Cambridge. He is currently a Professor with the Department of Modern Mechanics, University of Science and Technology of China. His research interests include the multiscale structured liquid metals composites and their applications in flexible electronics.

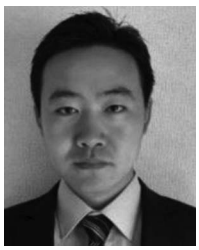

Shuaishuai Sun received the B.E. degree in mechanical engineering and automation from the China University of Mining and Technology, Beijing, China, in 2011, and the Ph.D. degree in mechanical engineering from the University of Wollongong, Wollongong, NSW, Australia, in 2016.

He is currently a Professor with the Department of Precision Machinery and Precision Instrumentation, University of Science and Technology of China, Hefei, China. He has authored and coauthored more than 120 journal articles in his research interests, which include intelligent mechanical and mechatronics systems, system dynamics, smart materials and structures, innovative actuators for locomotive robots, and vibration control.